



**HAL**  
open science

## The structure of human porphobilinogen deaminase at 2.8 Å: the molecular basis of acute intermittent porphyria

Raj Gill, Simon E. Kolstoe, Fiyaz Mohammed, Abeer Al D-Bass, Jonathan B. Cooper, Stephen P. Wood, Peter M. Shoolingin-Jordan

► **To cite this version:**

Raj Gill, Simon E. Kolstoe, Fiyaz Mohammed, Abeer Al D-Bass, Jonathan B. Cooper, et al.. The structure of human porphobilinogen deaminase at 2.8 Å: the molecular basis of acute intermittent porphyria. *Biochemical Journal*, 2009, 420 (1), pp.17-25. 10.1042/BJ20082077 . hal-00479112

**HAL Id: hal-00479112**

**<https://hal.science/hal-00479112>**

Submitted on 30 Apr 2010

**HAL** is a multi-disciplinary open access archive for the deposit and dissemination of scientific research documents, whether they are published or not. The documents may come from teaching and research institutions in France or abroad, or from public or private research centers.

L'archive ouverte pluridisciplinaire **HAL**, est destinée au dépôt et à la diffusion de documents scientifiques de niveau recherche, publiés ou non, émanant des établissements d'enseignement et de recherche français ou étrangers, des laboratoires publics ou privés.

## The Structure of Human Porphobilinogen Deaminase at 2.8 Å: The Molecular Basis of Acute Intermittent Porphyria

Raj Gill<sup>1</sup>, Simon E. Kolstoe<sup>1</sup>, Fiyaz Mohammed<sup>2</sup>, Abeer Al D-Bass, Jonathan B.Cooper<sup>1</sup>, Stephen P. Wood<sup>1</sup> & Peter M. Shoolingin-Jordan<sup>†</sup>

Biomolecular Sciences Group, School of Biological Sciences, University of Southampton, Bassett Crescent East, Southampton SO16 7PX, U.K.

<sup>1</sup> Current address: Centre for Amyloidosis and Acute Phase Proteins, Department of Medicine, UCL Medical School, Rowland Hill Street, London NW3 2PF, U.K.

<sup>2</sup> Current address: Cancer Research UK Institute for Cancer Studies, School of Cancer Sciences, University of Birmingham, Vincent Drive, Edgbaston, Birmingham B15 2TT, U.K.

**Abbreviations used:** CRIM, cross-reacting immunological material; CCD, charge-coupled device; DEAE, diethylaminoethyl; DTT, dithiothreitol; IPTG, isopropyl β D-thiogalactoside; NCS, non-crystallographic symmetry; PDB, protein data bank; PMSF, phenylmethanesulphonylflouride; RMSD, root mean square deviation; SDS-PAGE, sodium dodecyl sulphate – polyacrylamide gel electrophoresis.

<sup>†</sup> To whom correspondence should be addressed (pmsj@soton.ac.uk).

The Human uPBGD Structure has been submitted to the Protein Data Bank as 3eq1

## Abstract

Mutations in the human porphobilinogen deaminase gene cause the inherited defect, acute intermittent porphyria. Here we report the structure of the human ubiquitous porphobilinogen deaminase mutant, Arg167Gln, that has been determined by X-ray crystallography and refined to 2.8 Å resolution ( $R_{\text{factor}}=0.26$ ,  $R_{\text{free}}=0.29$ ). The protein crystallized in space group  $P2_12_12$  with two molecules in the asymmetric unit ( $a = 81.0$  Å,  $b = 104.4$  Å,  $c = 109.7$  Å). Phases were obtained by molecular replacement using the *E. coli* porphobilinogen deaminase structure as a search model. The human enzyme is composed of three domains each of approximately 110 amino acids and possesses a dipyrromethane cofactor at the active site which is located between domains 1 and 2. An ordered sulphate ion is hydrogen bonded to Arg<sup>26</sup> and Ser<sup>28</sup> at the proposed substrate binding site in domain 1. An insert of 29 amino acid residues, present only in mammalian porphobilinogen deaminase enzymes, has been modelled into domain 3 where it extends helix  $\alpha_3$  and forms a  $\beta$ -hairpin structure that contributes to a continuous hydrogen bonding network spanning domains 1 and 3. The structural and functional implications of the Arg167Gln mutation and other mutations that result in acute intermittent porphyria are discussed.

Accepted Manuscript

THIS IS NOT THE VERSION OF RECORD - see doi:10.1042/BJ20082077

## Introduction

Porphobilinogen deaminase (PBGD; EC 4.3.4.8, also referred to as hydroxymethylbilane synthase, preuroporphyrinogen synthase or uroporphyrinogen I synthase), is the third enzyme in the haem biosynthesis pathway in mammals [1]. The reaction catalysed by PBGD involves the formation of preuroporphyrinogen, a linear tetrapyrrole (bilane), by the extension of an enzyme-bound dipyrromethane (DPM) cofactor that acts as a reaction primer [2,3]. This is achieved by the sequential binding, deamination and condensation of four molecules of the substrate(S) porphobilinogen (PBG) through covalently bound enzyme (E) intermediates ES, ES<sub>2</sub>, ES<sub>3</sub> and ES<sub>4</sub> linked to the DPM cofactor. The resulting enzyme-bound hexapyrrole (ES<sub>4</sub>) is then hydrolysed, releasing the unstable tetrapyrrole product, preuroporphyrinogen (also called 1-hydroxymethylbilane) with regeneration of the enzyme with the DPM cofactor still bound at the active site.

PBGD possesses several novel features. Firstly, the initial protein translation product is an *apoenzyme* that has the ability to construct its own DPM cofactor using two of the pyrrole units of preuroporphyrinogen [4]. Secondly, each of the four substrate condensation steps occurs at a single catalytic site [5] and the enzyme is therefore able to translocate the growing polypyrrole chain to vacate the substrate binding site for the next incoming substrate. Thirdly, the enzyme can 'count' precisely to four and terminate the polymerisation reaction by hydrolysis when the hexapyrrole chain (ES<sub>4</sub>) has been assembled [3].

Comparison of the primary amino acid sequences of PBGDs from a wide range of organisms demonstrates a high degree of conservation (see Supplementary Data). For example, there is 60% similarity and 43% identity between the deaminases from *E. coli* and humans [6] (see Figure 1). PBGD from *E. coli* was the first haem biosynthesis enzyme structure to be solved, initially at 1.90 Å resolution [5] and subsequently refined to 1.76 Å [8]. The *E. coli* enzyme is composed of three  $\alpha/\beta$  domains of approximately equal size, linked together by flexible hinge regions. Domains 1 (*N*-terminal) and 2 are linked by two hinge segments and each possesses a similar fold based on a five-stranded, mixed  $\beta$ -sheet. There are relatively few direct interactions between the two domains which form an extensive active site cleft at their interface. Both domains 1 and 2 have the same overall topology as found in the transferrins and a number of bacterial periplasmic binding proteins which are known to adopt 'open' and 'closed' states in response to ligand binding [6]. Domain 3 (*C*-terminal) possesses an open-faced anti-parallel  $\beta$ -sheet of three strands, one face of which is covered by three  $\alpha$ -helices. A loop from domain 3 carries an invariant cysteine that forms the covalent attachment site for the dipyrromethane cofactor. Domain 3 interacts equally with both domains 1 and 2, the packing being mediated primarily through polar interactions of loop regions.

Mutations in human porphobilinogen deaminase cause acute intermittent porphyria (AIP), an inherited autosomal dominant disorder characterised by colicky abdominal pain and both peripheral and central neurological symptoms accompanied by elevated levels of the haem precursors 5-aminolevulinic acid (ALA) and porphobilinogen (PBG) in the urine. AIP is speculated to have been the cause of the madness of King George III [9]. In humans, alternative splicing of the PBGD mRNA gives rise to two monomeric *isozymes*, ubiquitous porphobilinogen deaminase (uPBGD) [10] that is expressed in all cells (361 residues; M<sub>r</sub> 39,620) and erythroid porphobilinogen deaminase (ePBGD) [11] which lacks the first 17 amino acids (344 residues; M<sub>r</sub> 38,120). To date, over 250 mutations resulting in human PBGD deficiency are listed in *The Human Gene Mutation Database Cardiff* (<http://www.hgmd.cf.ac.uk/ac/gene.php?gene=HMBS>) and references therein. Over one third of these mutations are nucleotide substitutions resulting either in single amino acid substitutions or premature chain termination. The likely impact of mutations on the structure

and activity of human PBGD was originally assessed from a homology model based on the *E. coli* enzyme structure [12,13], however, in regions of low homology and particularly in the vicinity of the 29 residue insert in the human enzyme sequence, a confident prediction of the functional consequences of mutations was not possible.

In this paper we present the X-ray structure of the Arg167Gln mutant of human ubiquitous PBGD. This was one of the first PBGD mutations to be identified [14] and is particularly interesting because the enzyme is weakly active (8.5%), has a reduced pH optimum and accumulates long-lived ES, ES<sub>2</sub>, ES<sub>3</sub> and ES<sub>4</sub> enzyme-intermediate complexes that are potentially able to provide information about the mechanism of pyrrole polymerisation.

Accepted Manuscript

## Materials and Methods

*Protein expression and purification.* Human uPBGD was expressed in *E. coli* strain BL21(DE3) pLysS following transformation with the pUHD2 plasmid, a derivative of pT7-7 [15]. The uPBGD insert in pUHD2 was constructed from a cDNA kindly provided by Professor Bernard Grandchamp (Paris). The Arg197Gln mutant of human porphobilinogen deaminase was constructed by site directed mutagenesis and expressed and purified using a purification procedure similar to that used for the native enzyme as described below [16].

Six 800 ml flasks containing 100 µg/ml ampicillin were inoculated with overnight cultures of transformed *E. coli* and grown at 37°C with shaking to an O.D.<sub>600</sub> of 0.6. IPTG was then added to 1 mM and bacterial growth continued for a further 3 hours. All subsequent steps were performed at 4°C except where noted. The cells were pelleted by centrifugation at 4,500 g, washed with 0.9M NaCl and recentrifuged. The bacterial pellet was then resuspended in 80 ml of 20 mM Tris.HCl buffer, pH 8.2, containing 5mM DTT, 200µM PMSF and sonicated for 20 cycles of 30 second bursts using an MSE Soniprep 150 sonicator, interspersed with periods of cooling for 90 seconds. The sonicate was placed in a flask filled with N<sub>2</sub> gas, heated rapidly to 60°C in a water bath for 10 minutes and then rapidly cooled to 4°C by immersion in an ice/water mixture with stirring. This heat treatment step inactivated uroporphyrinogen III synthase and removed a great deal of unwanted protein. The supernatant was then applied to a Pharmacia 50K/30 column packed with 150 ml of DEAE Sephacel anion-exchange resin which had been equilibrated in 50 mM Tris.HCl buffer, pH 8.2, containing 5 mM DTT and 100 µM PMSF. The column was washed with 1 L of the same buffer to remove unbound contaminating proteins. Bound proteins were eluted by the application of a linear KCl gradient (0-70 mM; 450 ml total volume at a flow rate of 0.35 ml/min). The deaminase was then eluted isocratically over approximately 100 ml at 70 mM KCl. Active fractions were pooled and concentrated to a final volume of 10 ml using an Amicon ultrafiltration cell (Millipore) fitted with a PM-10 membrane.

The deaminase, which was homogenous as judged by SDS-PAGE (not shown), was further concentrated to 1 ml using a Centricon YM-10 centrifugal filter (Millipore) and gel-filtered at 0.5 ml/minute on a Hiload™ 16/60 Superdex G-75 (Pharmacia) preparation grade column (120 x 1.6 cm) equilibrated in 100 mM Tris.HCl buffer, pH 8.2, containing 5 mM DTT and 100 µM PMSF. Peak fractions with enzymatic activity were pooled and concentrated to 1 ml using a Centricon YM-10. Finally, the deaminase was buffer-exchanged into 20 mM Tris.HCl buffer, pH 8.2, containing 5mM DTT, using a Pharmacia PD10 column. The specific activities of the purified recombinant wild-type and mutant uPBGD proteins were determined as described previously [17]. Protein concentrations were determined from the calculated extinction coefficient [18] ( $\epsilon_{280} = 0.40$  for a 0.1% solution).

*Protein crystallisation.* Human Arg167Gln uPBGD was crystallised using the vapour diffusion method [19]. Hanging drops were prepared by mixing equal volumes (4µl of protein solution (20 mg/ml in 20 mM Tris.HCl buffer, pH 8.2, containing 5mM DTT) and reservoir solution (0.6 M ammonium sulphate, 1.2 M lithium sulphate, 5% (v/v) ethylene glycol, 50 mM sodium citrate (pH 5.6) and 50 mM DTT). The hanging drops were equilibrated against 1 ml of reservoir solution and placed at room temperature in the dark.

*X-Ray data collection and processing.* Crystals of human Arg167Gln uPBGD were transferred from mother liquor to cryoprotectant (30% v/v glycerol) and flash-cooled in liquid ethane. Diffraction data were collected at the European Synchrotron Radiation Facility (ESRF Grenoble) at station BM14 linked to a MAR CCD detector at 100 K using an Oxford Cryosystems Cryostream cooler. A total of 180 0.5° oscillations were collected with an

exposure time of 120 seconds per frame at a crystal to detector distance of 145 mm. Intensity data was processed with MOSFLM [20] and sorted, scaled and merged using the Collaborative Computational Project 4 (CCP4) suite of programs [21].

*Structure determination and refinement.* The structure of human Arg167Gln uPBGD was solved by molecular replacement using the program MOLREP [22]. The search model consisted of the *E. coli* PBGD structure (PDB accession code 1PDA) with the DPM cofactor and water molecules omitted.

The model was refined using CNS [23] and PHENIX [24] with 21934 unique reflections in the 46.8 – 2.8 Å resolution range. The model was initially subjected to a round of rigid body refinement and torsion angle simulated annealing (slow cool from 5000-300 K in 25 K decrements) using CNS. This was followed by a number of rounds of model building in COOT [25], grouped B-factor, and restrained coordinate refinement in the program phenix.refine [26]. Two-fold NCS restraints, bulk solvent, and anisotropy correction were used throughout the restrained refinement process which was monitored using the  $R_{\text{factor}}$  and  $R_{\text{free}}$  statistics [27].

Accepted Manuscript

THIS IS NOT THE VERSION OF RECORD - see doi:10.1042/BJ20082077



## Results

*Specific Activity.* The specific activity at pH 8.0 of the purified Arg167Gln mutant deaminase was 0.12  $\mu$ moles of porphyrin formed per/mg/hr compared with the wild-type deaminase specific activity of 1.4  $\mu$ moles of porphyrin formed/mg/hr.

*X-ray structure analysis.* Thin colourless plate-like crystals grew after several weeks. The best crystal diffracted X-rays to a resolution of 2.8 Å and the space group was determined to be orthorhombic (space group  $P2_12_12$ ) with cell dimensions of  $a = 81.0\text{Å}$ ,  $b = 104.4\text{Å}$  and  $c = 109.7\text{Å}$ . The calculated crystal packing parameter  $V_M$ , assuming two uPBGD molecules (84 kDa) per asymmetric unit, is  $2.63 \text{Å}^3\text{Da}^{-1}$  which corresponds to a solvent content of 53% [28]. Although the data extended beyond 2.8 Å resolution, the intensity of the diffraction pattern for this crystal form was anisotropic (being particularly weak in the direction of the  $k$  reciprocal axis), nevertheless the completeness of the data with  $I/\sigma > 3$  was good.

The rotation function yielded two significant peaks at  $7.5\sigma$  and  $6.7\sigma$ , corresponding to the two molecules in the crystal asymmetric unit. The top rotation peak yielded a translation function peak of  $13.2\sigma$  with the next peak being at  $6.9\sigma$ . This solution was fixed and a second translation search was performed to determine the relative position of the second molecule, yielding a top peak of  $6.0\sigma$ , with a correlation coefficient of 0.43 and an  $R_{\text{factor}}$  of 0.52. Following the positioning of both molecules in the target asymmetric unit, the crystal packing of this solution was viewed using MOLPACK [29] and displayed sensible crystal contacts. Following rigid body refinement and simulated annealing, the  $R_{\text{factor}}$  dropped to 0.36 ( $R_{\text{free}}=0.40$ ). Initial examination of the averaged electron density maps revealed prominent  $F_o - F_c$  density for the DPM cofactor and for most of the 29 residue insert in domain 3, confirming the validity of the molecular replacement solution. The model was improved by manual rebuilding, during which the uPBGD residues were fitted to the  $2F_o - F_c$  density. 24 residues of the 29 residue insert in domain 3 and the DPM cofactor were built in during the later stages of refinement. Electron density was only visible from Val<sup>20</sup> onwards at the  $N$ -terminus and residues 56-76 of the active site loop were also disordered. This loop becomes disordered in some deaminase structures where the cofactor has become oxidised and the enzyme inactivated. Indeed, the rigid oxidised cofactor generally leads to a considerable improvement in crystal order. Nevertheless, the electron density here was of sufficient quality to build most of the human sequence into the map, to locate the cofactor and to establish the position and conformation of the 29 residue insert which is absent in the search model. The final structure was validated using PROCHECK [30] and MolProbity [31] and the coordinates deposited in the PDB as 3eq1. The final working  $R_{\text{factor}}$  was 0.26 ( $R_{\text{free}}=0.29$ ). The crystallographic data collection and refinement statistics are presented in Table 1.

*Overall structure.* The overall dimensions of the human uPBGD molecule are  $57 \times 43 \times 32 \text{Å}$ . The topologies of domain 1 (residues 20-115 and 214-238) and domain 2 (residues 116-213) are broadly similar with both consisting of a doubly wound, five stranded mainly parallel  $\beta$ -sheet (one strand is anti-parallel). The  $\alpha$ -helical segments pack against each face of the  $\beta$ -sheets. In contrast, domain 3 (residues 239-356) comprises an open faced three-stranded anti-parallel  $\beta$ -sheet with three  $\alpha$ -helical segments covering one of the faces. Figure 2a depicts the overall three-dimensional structure of human uPBGD and a topology diagram of the structure is presented in figure 2b.

Electron density is clearly present for 24 residues of the 29 residue insert (electron density was absent for residues 303 and 307-310) in domain 3, that is not present in the *E. coli* enzyme and which is positioned after strand  $\beta 3_3$  (residues 290-298). The polypeptide chain of



the human enzyme meanders away from the C-terminus of  $\beta_3$ , leading to a  $\beta$ -hairpin with residues 312-315 ( $\beta_4$ ) and residues 318-321 ( $\beta_5$ ) making up the antiparallel strands. Main chain hydrogen bonds (Leu<sup>315</sup>NH-Ile<sup>318</sup>CO and Leu<sup>315</sup>CO-Ile<sup>318</sup>NH) give way to a main chain-side chain interaction (Asp<sup>312</sup>CO-Arg<sup>321</sup>N $\epsilon$ ) as the strands diverge. The apical residue of the hairpin, Val<sup>316</sup>, hydrogen bonds through its carbonyl oxygen with the side chain of Arg<sup>251</sup>. The hairpin packs on top of  $\alpha_1$  (residues 241-256) and  $\alpha_3$  (residues 325-343) with hydrophobic side chains Leu<sup>315</sup>, Val<sup>316</sup>, Ile<sup>318</sup> and Ala<sup>320</sup> that protrude beneath the hairpin interacting with Leu<sup>329</sup>, Ile<sup>248</sup> and Leu<sup>244</sup> of the domain 3 helices. There are also a range of interactions between the hairpin and domain 1, in particular hydrogen bonds between the main chain atoms of the hairpin and the terminal residue of  $\beta_4$ , the last strand of domain 1 (Gly<sup>317</sup>CO-Ile<sup>110</sup>NH and Thr<sup>319</sup>NH-Ile<sup>110</sup>CO). This hydrogen bonding pattern comes close to defining an extended seven stranded sheet linking domains 1 and 3. Beyond the hydrogen-bonded region the relative strand twist is too large to define such a sheet formally. However, there are additional interactions, notably the Gln<sup>314</sup> side chain hydrogen bonds with the backbone carbonyl of Phe<sup>108</sup> and the OG atoms of Thr<sup>109</sup> and Thr<sup>319</sup> are hydrogen bonded with one another, further stabilising the interaction between domains 1 and 3. Following this excursion into the  $\beta$ -hairpin, helix  $\alpha_3$  (residues 325 to 343) extends for 19 residues (5 residues longer than the equivalent helix in the *E. coli* enzyme).

The  $\beta$ -hairpin is also involved in a range of packing interactions with neighbouring molecules in the crystal. The elongated loops that lead into the  $\beta$ -hairpin between strands  $\beta_4$  and  $\beta_5$  nestle in a solvent channel between two symmetry-related neighbours.

*Intermolecular contacts in the crystal.* Human uPBGD crystallizes with two molecules in the asymmetric unit, related by a local 2-fold axis. Both molecules interact through a substantial interface (1472 Å<sup>2</sup>) stabilised by a series of hydrophobic contacts and a number of salt bridges and hydrogen bonds (Figure 3). The contacts arise from helix  $\alpha_1$  (residues 29-46), the loop (residues 126-141) connecting strands  $\beta_5$  (residues 121-125) and  $\beta_1$  (residues 142-144), the C-terminal of helix  $\alpha_3$  and the preceding loop region (residues 189-196). Analysis by ProFace [32] demonstrates that the dimer interface area is only 5% of the total solvent accessible surface area of the individual protomers whereas the average value for a stable dimer is 16% [33]. Furthermore, the non-polar fraction of the interface area (881 Å<sup>2</sup>) accounts for only 14% of the fully buried atoms in the structure whereas the average value for a stable dimer is 65% [34]. Indeed there is no evidence to suggest the formation of stable dimers of human uPBGD upon gel filtration at neutral pH [35].

*Interactions between domains.* There are mainly polar contacts between the three domains in the human deaminase molecule suggesting a flexible structure similar to that proposed for *E. coli* PBGD [5]. With the exception of the main chain connection between domains 1 and 2, there is also a hydrophobic between Gln<sup>29</sup> and Met<sup>196</sup>. The 29 residue insert following the third strand in domain 3 ( $\beta_3$ ) which is absent in the *E. coli* deaminase structure is involved in packing against domain 1, the interaction being mediated primarily by hydrogen bonding.

In addition to the mainly hydrophilic interactions at the inter-domain regions of the human structure there are also several hydrophobic interactions. Residues at the interface between domains 1 and 3 include Leu<sup>97</sup>, Leu<sup>244</sup> and Cys<sup>247</sup> and, between domains 2 and 3 residues Ala<sup>152</sup>, Met<sup>212</sup> and Leu<sup>285</sup> are involved. The interface between domains 2 and 3 also contains the bulky aromatic Trp<sup>283</sup> that packs against Gln<sup>153</sup>.

*Structural comparison between human and E. coli PBGDs.* The three dimensional structure of human PBGD has many features in common with the *E. coli* PBGD structure, most notably the presence of three protein domains. The main differences between the human and *E. coli*

PBGD structures occur as insertions in loop regions. For example, there is a three residue insertion occurring between strands  $\beta 5_2$  and  $\beta 1_2$  (residues 129-131), a single residue insertion between helix  $\alpha 2_2$  and strand  $\beta 3_2$  (residue 180) and a 29 residue insertion between strand  $\beta 3_3$  and  $\alpha 2_3$  (residues 296-324). Of the 360 residues in human uPBGD there are only 148 sequence identities with the *E. coli* enzyme. These identities partly cluster around the active site but otherwise are distributed evenly over the protein structure. The differences are not especially concentrated in loop regions connecting secondary structure elements but often involve hydrophobic residues of the core. The close conservation of the tertiary structure is achieved by a subtle blend of compensatory substitutions arising from different parts of the sequence that come together in the fold.

Superposition of the conserved secondary structural regions of human uPBGD onto those of *E. coli* PBGD yields an RMSD of 0.97 Å over 160  $C_\alpha$  atoms. Superposition of individual domains demonstrates that domain 2 of the human uPBGD structure superposes well onto the corresponding domain of *E. coli* PBGD, yielding an RMSD of 0.61 Å (over 41  $C_\alpha$  atoms). Domains 1 and 3 yield RMSD of 0.75 Å (over 62  $C_\alpha$  atoms) and 0.81 Å (over 86  $C_\alpha$  atoms), respectively. When corresponding domains are individually overlaid, the other two domains are also well superposed, demonstrating that there is no major perturbation of domain relationships between the bacterial and human enzymes. However, inspection of the distribution of small structural differences in the overlays demonstrates that insertion of the  $\beta$ -hairpin motif between  $\beta 5_1$  in domain 1 and  $\alpha 1_3$  and  $\alpha 2_3$  in domain 3 interface has pushed these domains apart (figure 4).

The close equivalence of the *E. coli* and human enzyme structures demonstrated by their superposition implies that the volumes of their respective hydrophobic cores are very similar in spite of the many substitutions that occur in these regions. In domain 1, Leu<sup>6</sup>, Ile<sup>8</sup>, Ala<sup>20</sup>, Val<sup>36</sup>, Leu<sup>38</sup>, Ile<sup>77</sup>, Leu<sup>93</sup>, Ile<sup>203</sup>, Cys<sup>205</sup> and Leu<sup>216</sup> of *E. coli* PBGD are replaced by Ile<sup>21</sup>, Val<sup>23</sup>, Thr<sup>35</sup>, Phe<sup>51</sup>, Ile<sup>53</sup>, Leu<sup>92</sup>, Phe<sup>108</sup>, Val<sup>222</sup>, Val<sup>224</sup> and Val<sup>235</sup> respectively in the human uPBGD structure. In domain 2, Ile<sup>145</sup>, Val<sup>152</sup>, Tyr<sup>164</sup> and Leu<sup>179</sup> in the *E. coli* deaminase structure are substituted by Phe<sup>163</sup>, Leu<sup>170</sup>, Phe<sup>183</sup> and Trp<sup>198</sup> respectively in the human deaminase structure. In all cases where there is a substantial change in side chain volume, this is accompanied by compensatory changes and adjustments in adjacent residues. The majority of residues that contribute towards the hydrophobic core in domain 3 of the human enzyme possess small aliphatic side chains that are also conserved in the *E. coli* deaminase structure, occurring between two roughly parallel  $\alpha$ -helices ( $\alpha 1_3$  and  $\alpha 2_3$ ). There are two notable differences in this region, whereby Thr<sup>229</sup> and Met<sup>234</sup> in the *E. coli* PBGD structure are replaced by Ile<sup>248</sup> and Phe<sup>253</sup> respectively in the human uPBGD structure. Side chain substitution patterns at domain interfaces are similarly compensatory and contribute to the conservation of domain relationships.

*The active site of human uPBGD and the impact of the Gln167 mutation*. The active site cleft (15 x 13 x 12 Å) containing the DPM cofactor is located at the interface between domains 1 and 2 in a similar arrangement to that in the *E. coli* enzyme (Figure 5). The DPM cofactor is covalently bound to the protein via a thioether linkage with Cys<sup>261</sup>, a residue in a type-I turn in the sequence Gly,Gly,Cys,Ser,Val,Pro (residues 259-264) located at the end of a loop connecting helix  $\alpha 1_3$  and strand  $\beta 1_3$  in domain 3. The electron density for the DPM cofactor indicates that it occupies the native reduced conformation, consistent with the colourless nature of the crystals. The majority of the cofactor interactions with the protein are conserved between the human and *E. coli* enzymes. The acetate and propionate moieties of the DPM cofactor contribute most of the ionic interactions and hydrogen bonds to neighbouring active site side chains (Figure 5). The interactions between the carboxylate groups of ring C1 and the enzyme involve several invariant arginine residues (Arg<sup>149</sup>, Arg<sup>150</sup> and Arg<sup>173</sup>), the backbone

amide nitrogen of Ser<sup>146</sup> and the hydroxyl and backbone carbonyl group of Ser<sup>147</sup>. The DPM cofactor ring C2 is positioned towards the back of the active site cleft and interacts with Ser<sup>96</sup> and the backbone amide nitrogens of both Ala<sup>189</sup> and Gly<sup>218</sup>. The invariant Lys<sup>98</sup> and Asp<sup>99</sup> residues interact with both C1 and C2 rings; Lys<sup>98</sup> forming salt-bridges with the acetate cofactor side-chains, whereas a carboxylate oxygen of the catalytic Asp<sup>99</sup> hydrogen bonds to both pyrrole NH atoms of the DPM cofactor.

A prominent peak of electron density was observed within hydrogen bonding distance of Arg<sup>26</sup> and Ser<sup>28</sup> within the active site region and this has been refined as a sulphate ion derived from the crystal mother liquor (Figure 5). This site is occupied by the DPM ring C2 propionate in *E. coli* PBGD when the cofactor is in the oxidized linear conformation, and ring C2 occupies the proposed substrate binding site [5]. When this site is vacant in the reduced *E. coli* enzyme, an acetate ion, again derived from the crystal mother liquor, is found at the equivalent position as the sulphate ion observed here [8]. The electron density for the mutated Gln<sup>167</sup> side chain is poorly resolved in the absence of stabilising interactions with the protein or the cofactor, as is the case for the Arg<sup>149</sup> side chain in the reduced *E. coli* structure [36].

Figure 6 illustrates the remarkable stability of enzyme intermediate complexes in the case of the Arg167Gln mutant that hinders the turnover to form product and the regeneration of the free enzyme. These intermediates can be visualized if the samples are separated by non denaturing gel electrophoresis at 4 °C.

Accepted Manuscript

## Discussion

Human uPBGD consists of three domains, as is the case with the prokaryotic enzyme, but is slightly larger owing to an *N*-terminal extension of 17 amino acids, a 29 residue insertion in domain 3 and several elongated loop regions. The enzyme crystallised with the DPM cofactor in the native reduced conformation with an ordered sulphate ion hydrogen bonded to Arg<sup>26</sup> and Ser<sup>28</sup> at the proposed substrate binding site.

The electron density map allowed modelling of 24 residues of the 29 residue insert in domain 3 of human uPBGD (residues 296-324) that is not present in the *E. coli* enzyme and is positioned after strand  $\beta_3$ . This insert elongates helix  $\alpha_2$  and extends into a  $\beta$ -hairpin (strands  $\beta_4$  and  $\beta_5$ ) and comes close to forming an extended seven stranded sheet linking domains 1 and 3. Because of low sequence homology in this region the insert had previously been modelled before strand  $\beta_3$  at residue positions 289-317. Although the insert is distant from the active site, its interaction with domain 1 may modulate conformational fluctuations associated with enzyme action and perhaps promote the weak dimerisation exhibited in the crystal. Although human uPBGD crystallized with two monomers in the asymmetric unit, the dimer interface is not as extensive as seen in stable (physiological) dimers of other proteins, and there is no evidence to suggest the formation of dimeric human uPBGD at neutral pH in solution. However, the possibility of a weak interaction between subunits of the human enzyme cannot be excluded, perhaps playing a role in the channelling of the unstable preuroporphyrinogen product to uroporphyrinogen III synthase or some other regulatory process.

In humans the rate limiting reaction in haem biosynthesis is governed by 5-aminolaevulinate synthase (ALAS), the first enzyme of the eight step Shemin pathway [37]. Subsequently PBGD has the lowest specific activity, but under normal conditions 50% of the enzyme is adequate to sustain normal demands for haem. However under conditions where the demand for haem is high, the induction of ALAS is triggered. Any compromise in the activity of PBGD therefore results in the accumulation of the immediate precursors, ALA and PBG, and may precipitate an attack of acute intermittent porphyria (AIP).

The human uPBGD structure facilitates an understanding of the large number of inherited mutations that result in AIP. The original homology model of human PBGD based upon the *E. coli* PBGD X-ray structure [12,13] yielded structural insight into how the many AIP-associated mutations could affect enzyme activity. Interestingly, many of the porphyria-associated mutation sites are sites that also differ between the human and *E. coli* deaminases. However, in the human PBGD structure these isolated AIP associated substitutions cannot sustain the active form of the enzyme.

The Arg167Gln mutation is of particular interest since it provides insight into important aspects of the pyrrole polymerisation mechanism. The mutant enzyme is weakly active in samples taken from human blood and the recombinant human enzyme expressed in *E. coli* also exhibits an enzymatic activity of only 5-10% of that of the native enzyme [34]. The Arg167Gln uPBGD structure presented here demonstrates that the considerable loss of activity associated with this mutation arises from a discrete perturbation of the enzyme mechanism rather than from any major structural perturbation. Most interestingly, when incubated with PBG the Arg167Gln mutant generates stable catalytic intermediates (ES, ES<sub>2</sub>, ES<sub>3</sub> and ES<sub>4</sub>), whereas the native enzyme turns these intermediates over rapidly. Accordingly, the Arg167Gln mutant is CRIM +ve, reflecting the accumulation of these substantially longer lived enzyme intermediate complexes. Arg<sup>167</sup> is thought to play a key role in deaminase binding to PBG by breaking the internal salt bridge between the amino and acetic acid side chains of the unbound substrate. The combination of Asp<sup>99</sup> and Arg<sup>167</sup> may facilitate the cleavage of the intra-molecular salt bridge to form new interactions, the substrate



amino group interacting with Asp<sup>99</sup> and the substrate acetate group interacting with Arg<sup>167</sup>. It has previously been observed that the equivalent Arg<sup>149</sup> residue of the *E. coli* enzyme is well ordered only when interacting with the acetate side chain of a pyrrole bound at the proposed substrate binding site [5]. The proposed role of Arg<sup>167</sup> in breaking the intra-molecular salt bridge in the PBGD substrate would account for the lowering of the pH optimum of human uPBGD from pH 8 to pH 6 when it is substituted by Gln, since the salt bridge is much weaker at lower pH and can break without the assistance of the enzyme. The structure presented here suggests that the mechanistic lesions associated with this mutation are only felt when the Arg<sup>167</sup> side chain is required to visit the substrate site. Additionally, activity may also be reduced by the neutral Gln<sup>167</sup> side chain disrupting the positively charged active site surface over which the negatively charged polypyrrole chain may “slide” during polymerisation.

PBGD mutations associated with porphyria are widely dispersed over all three domains of the enzyme structure. Over a hundred of these mutations involve single base changes that result in the substitution of one amino acid residue for another (missense – summarised in fig1) or the formation of a truncated protein (nonsense) and it is the former group that is especially interesting for providing structure/function information for the enzyme. While the Arg167Gln mutation discussed above exemplifies those affecting pyrrole polymerisation, mutations that lead to attacks of AIP may be divided into three more broad groups according to their molecular basis, including mutations that affect protein stability and folding, cofactor assembly and the catalytic process.

Mutations of residues that are essential for protein folding and stability include those occurring in the hydrophobic core, in tight turns and other conformationally restricted areas. Their mutation may result in an abnormally folded or unstable protein that is rapidly degraded *in vivo*. Such proteins typically exhibit cross reacting immunological material phenotype (CRIM –ve) with antibody raised against the native protein. Because of their intrinsic instability it is not possible to study the equivalent recombinant proteins *in vitro*, however the impact of the mutation may be assessed by inspecting its location in the human uPBGD structure. For example, Leu<sup>245</sup> is a conserved buried hydrophobic side chain that interacts with a cluster of proline residues (Pro<sup>241</sup>, Pro<sup>302</sup>, Pro<sup>327</sup>) in domain 1. Substitution of Leu<sup>245</sup> by the AIP associated Arg<sup>245</sup> would bury a large positively charged side chain with resulting adverse consequences for the stability of the domain fold.

Clearly, mutations that lead to the premature introduction of a stop codon will result in a truncated protein, affecting both folding and stability. For example, the most common mutation within the PBGD gene in Swedish patients (Trp198Term) results in a severely truncated, probably inactive, and easily degraded protein, with patients exhibiting a CRIM –ve phenotype [38]. The incidence of attacks of AIP in patients carrying this lesion is one of the highest, considering the low penetrance (8%) of the disease [39]. Two truncating AIP associated mutations also target the domain 3 insert (Gln296Term and Gln314Term) and both of these would be expected to destabilise domain 3 and interfere with the correct folding of the enzyme during biosynthesis.

Other mutations do not adversely affect *apoenzyme* formation but do prevent the binding, reaction and assembly of the cofactor precursor preuroporphyrinogen (1-hydroxymethylbilane). In the absence of the stabilising influence of the DPM cofactor, the intrinsically unstable *apoenzyme* is denatured and broken down intracellularly. The importance of the DPM cofactor not only for enzyme activity but also for enhancing the stability of the protein is exemplified by the dramatic finding that the *apoenzyme* is rapidly denatured at 60°C whereas the *holoenzyme* loses little activity over 15 minutes at this temperature [40]. A close inspection of the structure in the vicinity of the cofactor demonstrates that it makes some 25 direct contacts with the protein. Phenotypes in this class are therefore normally CRIM -ve and include, for example, the well characterised “base 500

mutations" that target Arg<sup>149</sup> (Arg149Gln and Arg149Leu), a residue intimately involved in cofactor assembly. Expression of recombinant Arg149Gln human uPBGD in *E. coli* yields apoprotein with less than 5% of wild-type activity in crude extracts and which is heat labile and completely inactive after purification [41]. A negative reaction with Ehrlich's reagent [17] confirmed that the purified mutant is devoid of the DPM cofactor and furthermore, attempts to incorporate preuroporphyrinogen *in vitro* were unsuccessful [34].

Finally, mutations that affect catalytic residues or substrate binding residues result in a correctly folded but inactive enzyme. Mutations at the substrate binding site include Arg26His and Arg173Gln. Mutagenesis studies at the equivalent positions in the *E. coli* enzyme (Arg11His and Arg155His [42] or Arg11Leu and Arg155Leu [43]) demonstrate that these mutations prevent the enzyme from binding substrate. Both of these human mutant PBGDs appear to be correctly folded since they exhibit a CRIM +ve phenotype and contain the DPM cofactor. However the disruption of the porphobilinogen binding site clearly prevents ES complex formation and both mutants are essentially inactive. Mutations involving the catalytic Asp<sup>99</sup> are of particular interest since they trap the deaminase in the ES<sub>2</sub> form. Although reaction of Asp99Gly human uPBGD apoenzyme with the tetrapyrrole cofactor precursor, preuroporphyrinogen, appears to be unaffected, the resulting ES<sub>2</sub> complex is unable to catalyse the addition of further substrate to complete the catalytic cycle and generate the product and the DPM cofactor [44]. The related Asp84Ala mutation in *E. coli* PBGD also appears to exist as an inactive ES<sub>2</sub> complex [45]. Both findings support the hypothesis that the cofactor arises not from two single molecules of substrate but from a preformed tetrapyrrole [4].

All of these mutants of human PBGD have been identified on the basis that their *in vivo* activity is low enough to cause symptoms of AIP. When the CRIM status confirms that normal amounts of enzyme are produced, these mutations provide an informative repertoire of lesions in protein function that contribute towards a deeper understanding of the enzyme's mechanism of action.



### Acknowledgements

We are grateful to Professor Joël Janin (Laboratoire d'Enzymologie et Biochimie Structurales, Centre National De La Recherche Scientifique, Paris, France) and Dr Ranjit Bahadur (Department of Biochemistry, Bose Institute, Kolkata, India) for running the dimer interface calculations and to Dr M. Sarwar for constructing the human uPBGD expression clones. Mr Barry Lockyer kindly assisted with the production of the figures.

Accepted Manuscript

THIS IS NOT THE VERSION OF RECORD - see doi:10.1042/BJ20082077

## References

1. Shoolingin-Jordan, P.M. and Cheung, K.-M. (2000) Biosynthesis of heme. In *Comprehensive Natural Products Chemistry*, Volume 4 (Barton, D.H.R., and Nakanishi, K., ed.), pp. 61-107, Pergamon/Elsevier, New York
2. Jordan, P.M. and Warren, M.J. (1987) Evidence for a dipyrromethane cofactor at the catalytic site of *E. coli* porphobilinogen deaminase. *FEBS Lett.* **225**, 87-92
3. Warren, M.J. and Jordan, P.M. (1988) Investigation into the nature of substrate binding to the dipyrromethane cofactor of *E. coli* porphobilinogen deaminase. *Biochemistry* **27**, 9020-9030
4. Shoolingin-Jordan, P.M., Warren, M.J. and Awan, S.J. (1996) Discovery that the assembly of the dipyrromethane cofactor of porphobilinogen deaminase *holoenzyme* proceeds initially by the reaction of preuroporphyrinogen with the *apoenzyme*. *Biochem. J.* **316**, 373-376
5. Louie, G.V., Brownlie, P.D., Lambert, R., Cooper, J.B., Blundell, T.L., Wood, S.P., Warren, M.J., Woodcock, S.C. and Jordan, P.M. (1992) Structure of porphobilinogen deaminase reveals a flexible multidomain polymerase with a single catalytic site. *Nature* **359**, 33-39
6. Louie, G.V. (1993) Porphobilinogen deaminase and its structural similarity to the bidomain binding proteins. *Curr. Opin. Struct. Biol.* **3**, 401-408
7. Barton, G. J. (1993) ALSCRIPT: A tool to format multiple sequence alignments. *Protein Eng.* **6**, 37-40
8. Louie, G.V., Brownlie, P.D., Lambert, R., Cooper, J.B., Blundell, T.L., Wood, S.P., Malashkevich, V.N., Hädener, A., Warren, M.J. and Jordan, P.M. (1996) The three-dimensional structure of *Escherichia coli* porphobilinogen deaminase at 1.76Å resolution. *Protein. Struct. Funct. Genet.* **25**, 48-78
9. Röhl, J.C.G., Warren, M.J. and Hunt, D. (1998) *Purple Secret: Genes, "Madness" and the Royal Houses of Europe*, Bantam Press, London
10. Grandchamp, B., De Verneuil, H., Beaumont, C., Chretien, S., Walter, O. and Nordmann, Y. (1987) Tissue-specific expression of porphobilinogen deaminase: Two *isoenzymes* from a single gene. *Eur. J. Biochem.* **162**, 105-110
11. Raich, N., Romeo, P.H., Dubart, A., Beaupain, D., Cohen-Solal, M. and Goossens, M. (1986) Molecular cloning and complete primary sequence of human erythrocyte porphobilinogen deaminase. *Nucleic Acids Res.* **14**, 5955-5968
12. Brownlie, P.D., Lambert, R., Louie, G.V., Jordan, P.M., Blundell, T.L., Warren, M.J., Cooper, J.B. and Wood, S.P. (1994) The three-dimensional structures of mutants of porphobilinogen deaminase: Toward an understanding of the structural basis of acute intermittent porphyria. *Protein. Sci.* **3**, 1644-1650

13. Wood, S.P., Lambert, R. and Jordan, P.M. (1995) Molecular basis of acute intermittent porphyria. *Mol. Med. Today* **1**, 232-239
14. Delfau, M.H., Picat, C., de Rooij, F.W., Hamer, K., Bogard, M., Wilson, J.H., Deybach, J.C., Nordmann, Y. and Grandchamp, B. (1990) Two different point G to A mutations in exon 10 of the porphobilinogen deaminase gene are responsible for acute intermittent porphyria. *J. Clin. Investig.* **86**, 1511-1516
15. Tabor, S. and Richardson, C.C. (1985) A bacteriophage T7 RNA polymerase/promoter system for controlled exclusive expression of specific genes. *Proc. Natl. Acad. Sci. U.S.A.* **82**, 1074-1078
16. Jordan, P.M., Thomas, S.D. and Warren, M.J. (1988) Purification, crystallization and properties of porphobilinogen deaminase from a recombinant strain of *Escherichia coli* K12. *Biochem. J.* **254**, 427-435
17. Shoolingin-Jordan, P.M., Warren, M.J. and Awan, S.J. (1997) Dipyrrromethane cofactor assembly; Formation of *apoenzyme* and preparation of *holoenzyme*. In: *Methods. Enzymol.* **281** (McCormick, D.B., Suttie, J.W. and Wagner, C. ed.), pp 317-327, Academic Press, London
18. Gill, S.C. and von Hippel, P.H. (1989) Calculation of protein extinction coefficients from amino acid sequence data. *Anal. Biochem.* **182**, 319-326
19. Macpherson, A. (1982) *Preparation and Analysis of Protein Crystals*, John Wiley and Sons, New York
20. Leslie, A.G.W. (1992) Joint CCP4 and ESF-EACMB newsletter on protein crystallography No 26, Daresbury laboratory, Warrington, UK
21. Collaborative Computational Project, Number 4 (1994) The CCP4 suite: Programs for protein crystallography. *Acta Crystallogr.* **D50**, 760-763
22. Vagin, A. and Teplyakov, A. (1997) MOLREP: An automated program for molecular replacement. *J. Appl. Crystallogr.* **30**, 1022-1025
23. Brünger, A.T., Adams, P.D., Clore, G.M., DeLano, W.L., Gros, P., Grosse-Kunstleve, R.W., Jiang, J.S., Kuszewski, J., Nilges, M., Pannu, N.S., Read, R.J., Rice, L.M., Simonson, T. and Warren, G.L. (1998) Crystallography & NMR system: A new software suite for macromolecular structure determination. *Acta Crystallogr.* **D54**, 905-921
24. Adams, P.D., Grosse-Kunstleve, R.W., Hung, L.-W., Ioerger, T.R., McCoy, A.J., Moriarty, N.W., Read, R.J., Sacchettini, J.C., Sauter, N.K. and Terwilliger, T.C. (2002) PHENIX: Building new software for automated crystallographic structure determination. *Acta Crystallogr.* **D58**, 1948-1954
25. Emsley, P. and Cowtan, K. (2004). *Coot*: model-building tools for molecular graphics. *Acta Crystallogr.* **D60**, 2126-2132

26. Afonine, P.V., Grosse-Kunstleve, R.W. and Adams, P.D. (2005) The Phenix refinement framework. *CCP4 Newsletter* **42**, contribution 8
27. Brünger, A.T. (1992) Free R value: A novel statistical quantity for assessing the accuracy of crystal structures. *Nature* **355**, 472-475
28. Mathews, B.W. (1968) Solvent content of protein crystals. *J. Mol. Biol.* **33**, 491-497
29. Wang, D.W., Driessen, H.P. and Tickle, I.J. (1991) MOLPACK: Molecular graphics for studying the packing of protein molecules in the crystallographic unit cell. *J. Mol. Graph.* **9**, 50-52
30. Laskowski, R.A., MacArthur, M.W., Moss, D.S. and Thornton, J.M. (1993) PROCHECK: A program to check the stereochemical quality of protein structures. *J. App. Crystallogr.* **26**, 283-291
31. Lovell, S.C., Davis, I.W., Arendall, W.B., de Bakker, P.I.W., Word, J.M., Prisant, M.G., Richardson, J.S. and Richardson, D.C. (2003) Structure validation by  $C\alpha$  geometry:  $\phi, \psi$  and  $C\beta$  deviation. *Protein. Struct. Funct. Genet.* **50**, 437-450.
32. Saha R. P., Bahadur R. P., Pal A., Mandal S. and Chakrabarti P. (2006). ProFace: A server for the analysis of the physicochemical features of protein-protein interfaces. *BMC Struct. Biol.* **6**: 11.
33. Bahadur, R.P., Chakrabarti, P., Rodier, F. and Janin, J. (2003) Dissecting subunit interfaces in homodimeric proteins. *Protein. Struct. Funct. Genet.* **53**, 708-719
34. Bahadur, R.P., Chakrabarti, P., Rodier, F. and Janin, J. (2004) A dissection of specific and non-specific protein-protein interfaces. *J. Mol. Biol.* **336**, 943-955
35. Al-Dbass, A. (2001) Structural basis of acute intermittent porphyria and the relationship between mutations in human porphobilinogen deaminase and enzyme activity. Ph.D. Thesis, University of Southampton
36. Hädener, A., Matzinger, P.K., Battersby, A.R., McSweeney, S., Thompson, A.W., Hammersley, A.P., Harrop, S.J., Cassetta, A., Deacon, A., Hunter, W.N., Nieh, Y.P., Raftery, J., Hunter, N. and Helliwell, J.R. (1999) Determination of the structure of selenomethionine-labelled hydroxymethylbilane synthase in its active form by multi-wavelength anomalous dispersion. *Acta Crystallogr.* **D55**, 631-643
37. Thunell (2000) Porphyrins, porphyrin metabolism and porphyrias I. Update. *Scand. J. Clin. Lab. Investig.* **60**, 509-540
38. Lee, J.-S. and Anvert, M. (1991) Identification of the most common mutation within the porphobilinogen deaminase gene in Swedish patients with acute intermittent porphyria. *Proc. Natl. Acad. Sci. U.S.A.* **88**, 10912-10915
39. Andersson, C., Floderus, Y., Wikber, A. and Lithner, F. (2000) The W198X and R173W mutations in the porphobilinogen deaminase gene in acute intermittent porphyria have higher clinical penetrance than R167W. A population-based study. *Scand. J. Clin. Lab. Investig.* **60**, 643-648

40. Awan, S.J., Siligardi, G., Shoolingin-Jordan, P.M. & Warren, M.J. (1997) Reconstitution of the *holoenzyme* form of *Escherichia coli* porphobilinogen deaminase from apoenzyme with porphobilinogen and preuroporphyrinogen: A study using circular dichroism spectroscopy. *Biochemistry* **36**, 9273-82
41. Shoolingin-Jordan, P.M. *Unpublished*
42. Jordan, P. and Woodcock, S.C. (1991) Mutagenesis of arginine residues in the catalytic cleft of *Escherichia coli* porphobilinogen deaminase that affects dipyrromethane cofactor assembly and tetrapyrrole chain initiation and elongation. *Biochem. J.* **280**, 445-449
43. Lander, M., Pitt, A.R., Alefounder, P.R., Bardy, D., Abell, C. and Battersby, A.R. (1991) Studies on the mechanism of hydroxymethylbilane synthase concerning the role of arginine residues in substrate binding. *Biochem. J.* **275**, 447-452
44. Shoolingin-Jordan, P.M., Al-Dbass, A., McNeill, L.A., Sarwar, M. and Butler, D. (2003) Human porphobilinogen deaminase mutations in the investigation of the mechanism of dipyrromethane cofactor assembly and tetrapyrrole formation. *Biochem. Soc. Trans.* **31**, 731-735
45. Woodcock, S.C. and Jordan, P.M. (1994) Evidence for participation of aspartate-84 as a catalytic group at the active site of porphobilinogen deaminase obtained by site-directed mutagenesis of the *hemC* gene from *Escherichia coli*. *Biochemistry* **33**, 2688-2695
46. Larkin, M.A., Blackshields, G., Brown, N.P., Chenna, R., McGettigan, P.A., McWilliam, H., Valentin, F., Wallace, I.M., Wilm, A., Lopez, R., Thompson, J.D., Gibson, T.J., Higgins, D.G. (2007) Clustal W and Clustal X version 2.0. *Bioinformatics* **23**, 2947-2948

Accepted Manuscript

## Figure legends

**Figure 1.** Structural alignment of the amino acid sequences of human uPBGD and *E.coli* PBGD. Identical residues are boxed and the secondary structural elements are coloured according to domain. N- and C-terminal residues, active site loop residues and the human domain 3 insert residues not visible in the electron density map are highlighted in grey. AIP associated single residue mutations are displayed beneath the human uPBGD sequence. Residues conserved across PBGDs from all species are indicated by ●, conserved substitutions are indicated by ○ and semi-conservative substitutions are indicated by ×. The sequence alignment was depicted with ALSCRIPT [7]. Amino acids are colour-coded such that red indicates acidic residues, blue basic, green neutral, pink hydrophobic, yellow cysteine and white indicates the conformationally important glycine, alanine and proline residues.

**Figure 2. (a)** The structure of human uPBGD with the three domains coloured differently; domain 1 (green), domain 2 (blue) and domain 3 (yellow). The dipyrromethane cofactor (red) and sulphate ion is located at the catalytic site between domains 1 and 2. **(b)** The topology of the secondary structure of human uPBGD. Domain 1 (green) extends from residues 20 to 115 and residues 214 to 238. Domain 2 (blue) is comprised of residues 116-213. Domain 3 (yellow) extends from residue 239 to residue 356 and contains the cofactor binding Cys<sup>261</sup> residue. The disordered residues (56-76) and the location of the DPM cofactor are indicated.

**Figure 3.** The two molecules of human uPBGD in the asymmetric unit. Although both molecules interact through a substantial interface stabilised by hydrophobic contacts, salt bridges and hydrogen bonds they probably do not constitute a physiological dimer.

**Figure 4.** Although the human (yellow) and *E. coli* (green) deaminase structures superpose well, the 29 residue domain 3 insert in the human enzyme (in blue) has pushed domains 1 and 3 apart. The dipyrromethane cofactor (red) is in the oxidized conformation in the *E. coli* deaminase structure but in the reduced conformation in the human deaminase structure.

**Figure 5.** The active site of human uPBGD with superposed electron density (omit map) contoured at  $2\sigma$ . The dipyrromethane (dpm) cofactor interacts with the protein through over 25 contacts, notably with the conserved Ser<sup>147</sup>, Arg<sup>150</sup> and Arg<sup>173</sup> residues. The catalytic Asp<sup>99</sup> is hydrogen bonded to both NH groups of the cofactor pyrrole rings and a sulphate ion is bound to Arg<sup>26</sup> and Ser<sup>28</sup> at the predicted substrate binding site.

**Figure 6.** Non-denaturing PAGE analysis demonstrating the stability of human uPBGD enzyme intermediate complexes generated upon incubation with substrate. Enzyme was either incubated with 10 mole equivalents of porphobilinogen at 37°C for a short period (a few seconds) in 20mM Tris/HCl buffer, pH 8, or the incubation was prolonged until reaction of the native enzyme had proceeded to completion (1 hour). All samples were cooled to 0°C and then loaded together at 4°C. Track 1, native enzyme; track 2, Arg167Gln mutant enzyme; track 3, native enzyme + porphobilinogen; track 4, Arg167Gln + porphobilinogen; track 5, sample from track 3 allowed to react to completion; track 6, sample from track 4 allowed to react to completion. (Note that the purified enzyme always exhibits 2 protein bands on non-denaturing PAGE; the most prominent enzyme intermediate complexes are ES<sub>2</sub> and ES<sub>3</sub>).



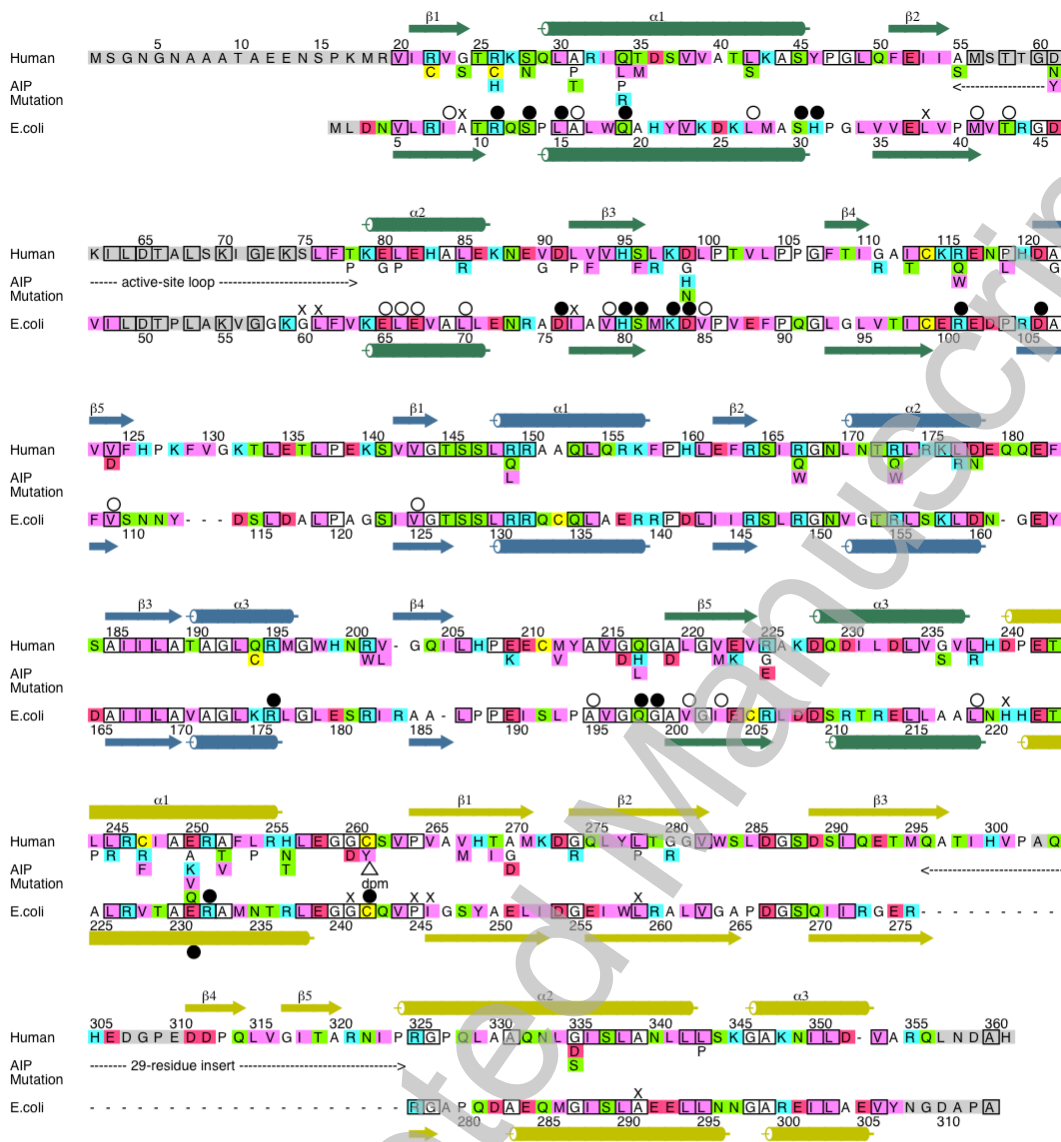
**Table 1**

Data-collection and refinement statistics for human uPBGD

Values in parentheses are for the outer shell.

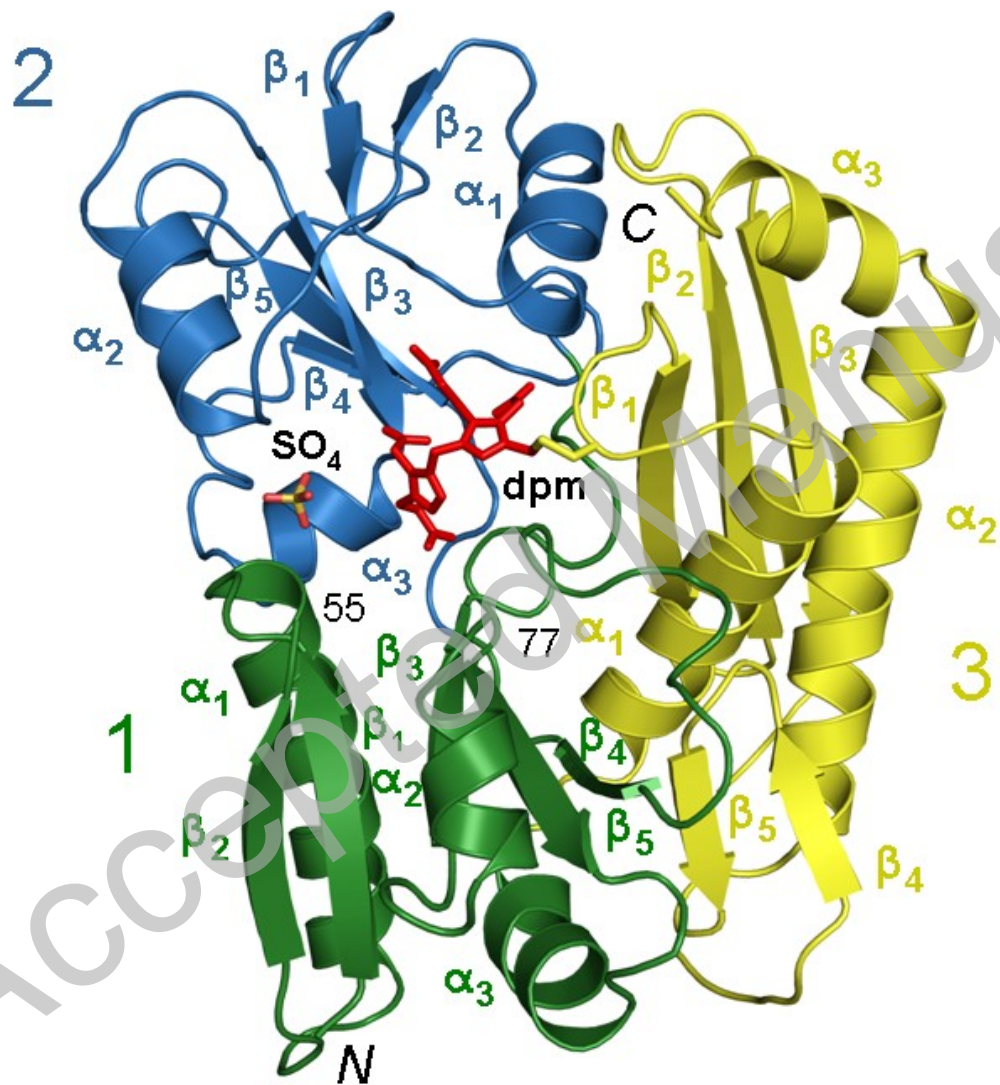
Unit cell and symmetry		
Radiation Source	ESRF BM14	
Radiation Wavelength (Å)	1.000	
Space Group	P2 <sub>1</sub> 2 <sub>1</sub> 2	
Unit-cell parameters		
<i>a</i> (Å)	81.03	
<i>b</i> (Å)	104.44	
<i>c</i> (Å)	109.73	
$\alpha$ (°)	90.00	
$\beta$ (°)	90.00	
$\gamma$ (°)	90.00	
Estimated solvent content (%)	53	
Subunits in AU	2	
Data Set Statistics		
Resolution range (Å)	46.8-2.8	(2.95-2.8)
Measured Reflections	83971	(12137)
Unique Reflections	21934	(3201)
$R_{\text{merge}}$	0.09	(0.47)
Completeness (%)	95.4	(96.4)
$\langle I/\sigma(I) \rangle$	13.2	(3.8)
Multiplicity	3.8	(3.8)
Wilson B-factor (Å <sup>2</sup> )	43.95	
Refinement Statistics		
$R_{\text{factor}}$	0.26	
$R_{\text{free}}$	0.29	
Number of reflections in free set	1711	
RMSD bond length (Å)	0.003	
RMSD bond angle (°)	0.658	
Number of protein atoms	4830	
Average B-factor protein (Å <sup>2</sup> )	64.01	
Residues in most favoured regions (%)	94.75	
Residues in additionally allowed regions (%)	5.25	
Residues in generously allowed regions (%)	0	

Figure 1



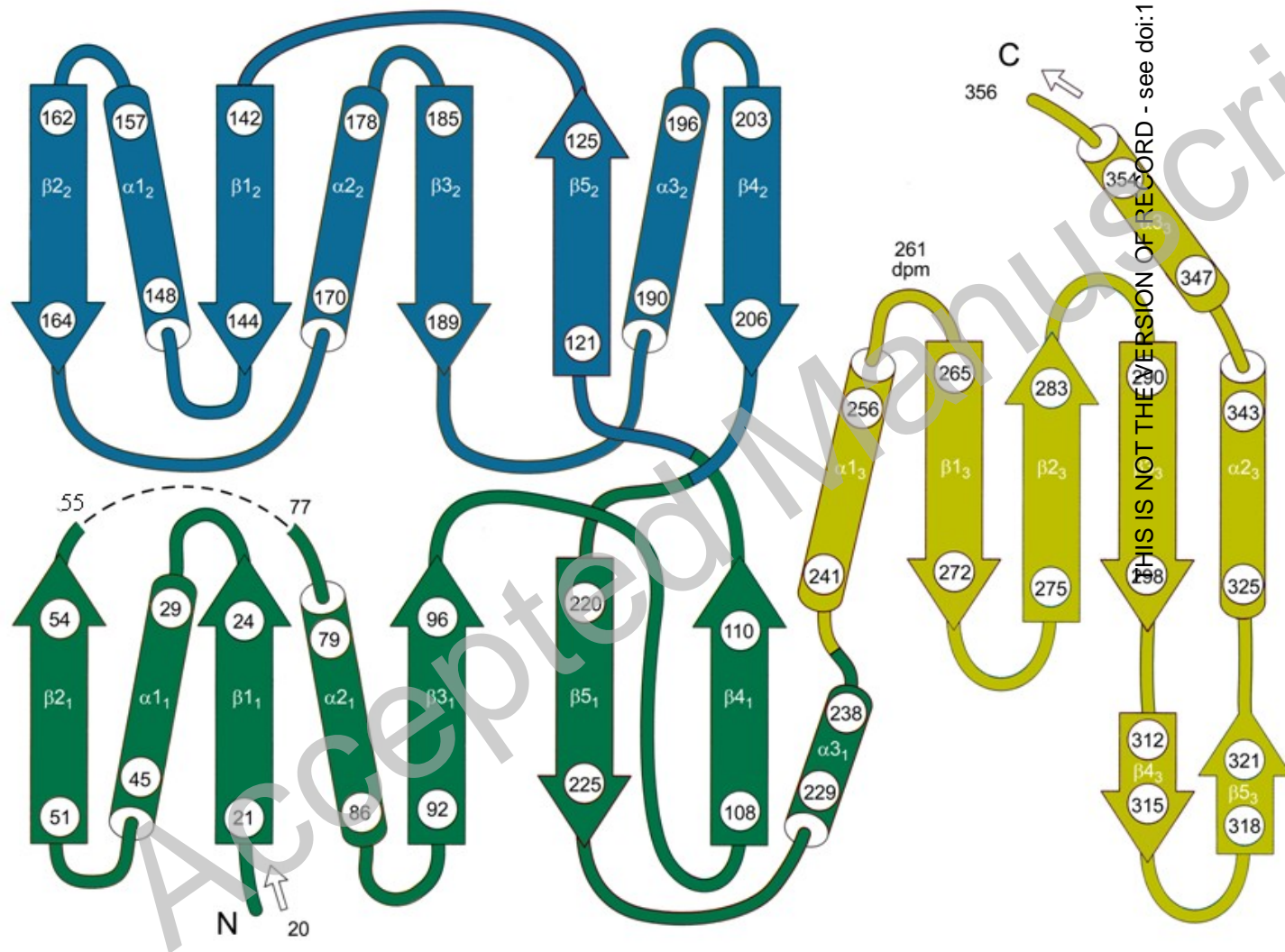
THIS IS NOT THE VERSION OF RECORD - see doi:10.1042/BJ20082077

Figure 2a

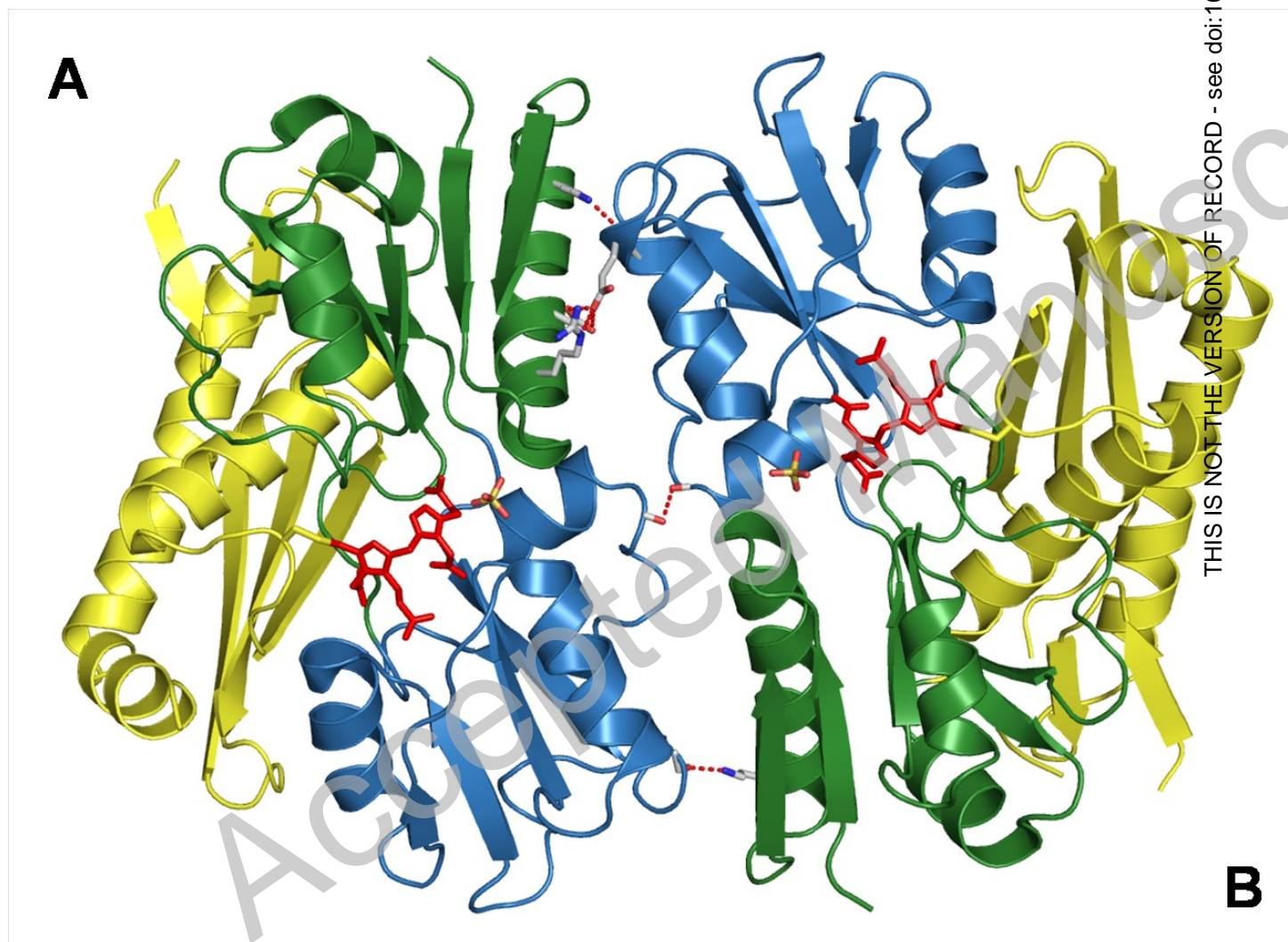


THIS IS NOT THE VERSION OF RECORD - see doi:10.1042/BJ20082077

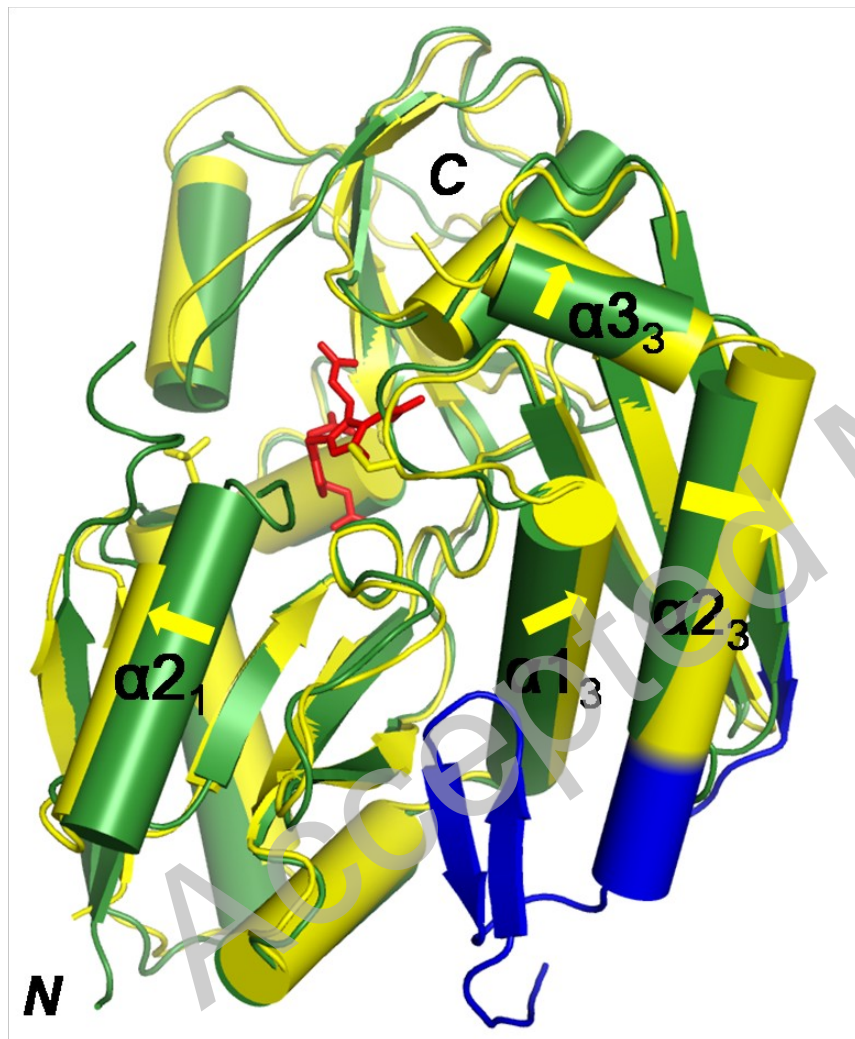
Figure 2b





**Figure 3**

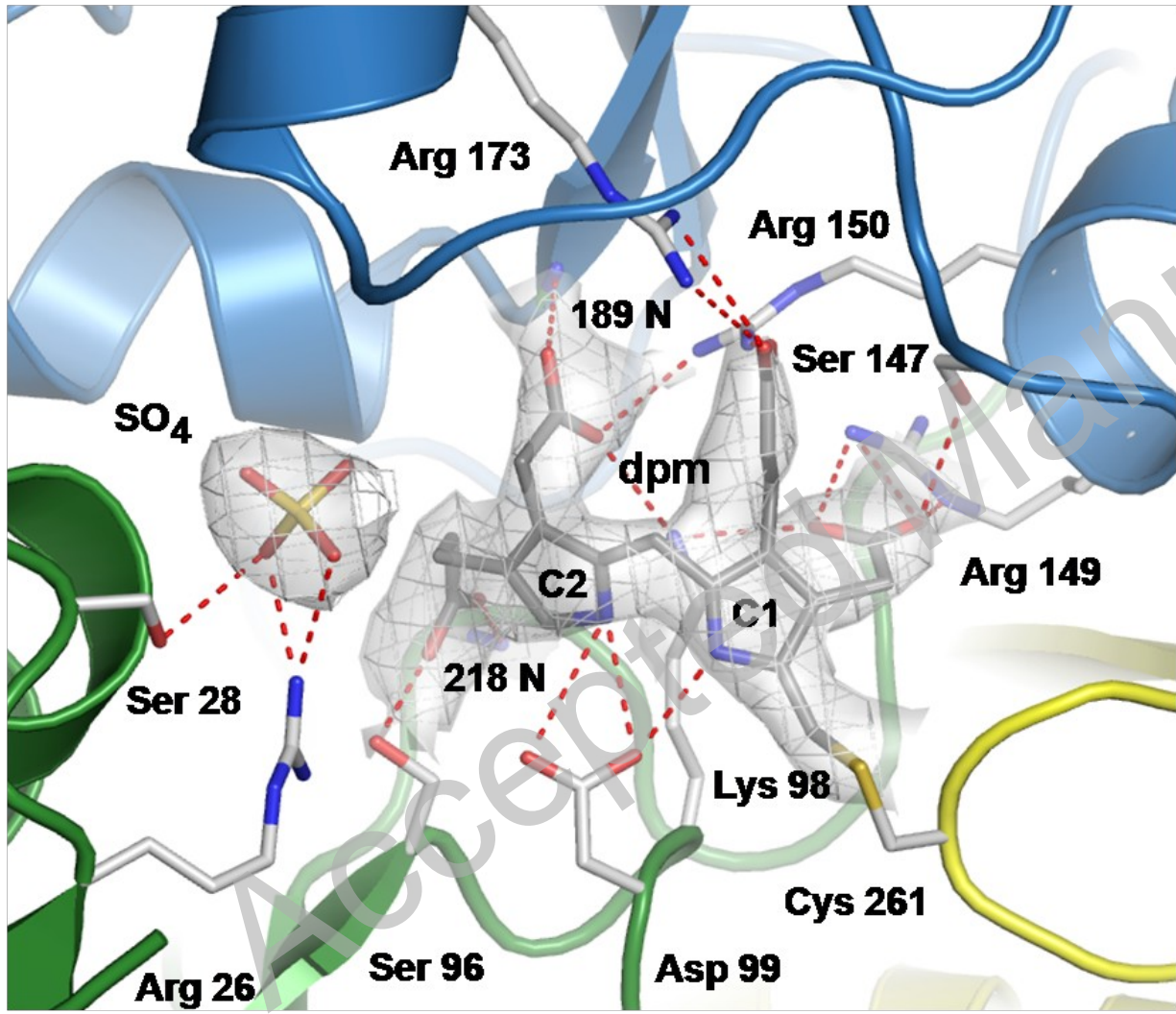
**Figure 4**



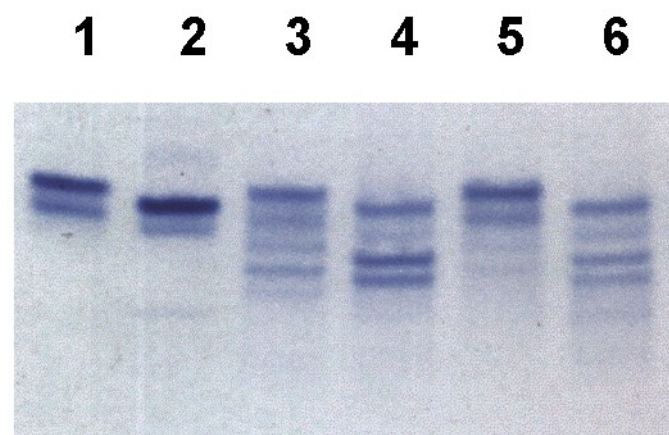
THIS IS NOT THE VERSION OF RECORD - see doi:10.1042/BJ20082077



Figure 5



THIS IS NOT THE VERSION OF RECORD - see doi:10.1042/BJ20082077

**Figure 6**

THIS IS NOT THE VERSION OF RECORD - see doi:10.1042/BJ20082077

Accepted Manuscript